HIGH PERFORMANCE SCANNING THERMAL PROBE USING A LOW TEMPERATURE POLYIMIDE-BASED MICROMACHINING PROCESS

M.-H. Li, J.J. Wu*, and Y.B. Gianchandani[1]

Center for Nano Technology, Department of Electrical and Computer Engineering,
University of Wisconsin, Madison, USA

ABSTRACT

This paper describes scanning thermal probes that exploit the low thermal conductivity and the high mechanical flexibility of polyimide as a structural material. They are surface micromachined using a low-temperature 6-mask process suitable for appending to a CMOS fabrication sequence. The probes are 200-1000 μm long, 40-120 μm wide, and of varying thickness. They are assembled by a flip-over approach that obviates the need for dissolving the substrate wafer or removing the probe from it. Temperature sensing is provided by thin-film Ni/W thermopiles embedded in the polyimide. Measurements indicate temperature sensitivity of 6 μV/K, and bandwidth of 500 Hz. Modeling results indicate that the polyimide provides almost 10x larger temperature sensitivity than a Si probe of equal dimensions. A sample scan is presented.

I. INTRODUCTION

Thermal probes are of increasing interest in a variety of applications, including high resolution temperature mapping (e.g., for ULSI diagnostics), topographical mapping, photothermal absorption spectroscopy, and subsurface imaging [Wic89, Ham96, Var98]. Two applications of particular interest to us are related to photolithography research: mapping the latent image in exposed but undeveloped photoresist, and micro-calorimetric analysis of sub-micron features of resist to determine the impact of spatial boundary conditions [Oco96, Fry98]. Thermal probes based on various temperature sensing techniques have been reported in the past: the commercially available Wollaston probe which reads out a resistance change in a bent wire; the coated wire thermocouple (TC) [Wil86]; micromachined thin-film TC's [Suz96, Luo97, Gia97, Mil98]; Schottky diodes [Lei98]; and Joule expansion [Maj98]. The Wollaston probe has a tip diameter in the range of 10-50 μm, whereas most of the other options offer tip diameters of 10 nm to 1 μm. The wire-based probes generally do not offer as much thermal isolation and reproducibility as the micromachined probes. For the purpose of integration with interface circuitry, the TC-based approaches offer an attractive compromise between fabrication simplicity and performance.

This effort describes a new type of TC-based thermal probe for scanning microscopy applications that is fabricated with a low-temperature, 6-mask process intended for ease of integration with CMOS circuitry. The probe has a built-in scanning tip that is exposed by a unique flip-over assembly step at the end of processing. The probe design allows it to be used for tunneling and force microscopy. Section II presents the structure and operation of the probe, section III describes the fabrication sequence, and section IV describes experimental results that have been obtained with this probe. Sample scans, temperature sensitivity, and response speed measurements are presented.

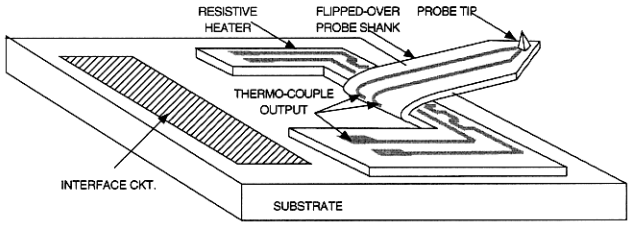

Fig. 1. Schematic of the thermal probe illustrating the flip-over approach for tip clearance.

II. STRUCTURE AND OPERATION

The structure of the polyimide-based thermal probe is illustrated in Fig. 1. A cantilever with a thin-film TC sandwiched between two layers of polyimide is released from the surface of the substrate wafer and flipped over to expose the scanning tip which initially pointing down. This tip clearance method exploits the flexibility of polyimide, and produces a structure that is in some ways similar to ciliary motion actuators [Ata93]. For increased temperature sensitivity the TC may be replaced by a thermopile. The TC has one junction located within the scanning tip, which is at the distal end of the cantilever, and while the other junction is located on unreleased polyimide at its base. The advantage of having a differential measurement from these two junctions, spaced apart only a few hundred microns, is that common mode errors results from convection or other effects are automatically cancelled out. The base of the probe incorporates a thin film resistor to provide an optional temperature bias between the proximal junction of the TC and the sample.

The flip-over method for providing the tip clearance obviates the removal of the substrate material from underneath the tip, which has been performed in the past but is not favored in the presence of on-chip circuitry [Suz96]. Moreover, the flip-over method extends the probe cantilever past the edge of the chip, allowing the

* Present affiliation: KLA Tencor Corporation, San Jose, California

[1] *Corresponding author*: 1415 Engineering Dr., UW-Madison, 53706-1691, USA; Tel: (608) 262-2233; Fax: 262-1267; yogesh@engr.wisc.edu

scanning tip to be visually aligned with the sample. This feature is also necessary to provide a clear optical path for the laser if the probe is to used for force microscopy [Aki99, Tha99]. Another possibility is to fabricate the probe pointing upwards on the substrate wafer [Mil98]. In this case the options for providing an optical path are once again to dissolve the substrate wafer near the probe head, or to remove the probe from the substrate entirely and relocate is elsewhere. Neither of these are attractive for an integrated solution.

The thermal probe may be operated in either contact mode, in which the tip is touching the sample, or in non-contact mode. The principle of non-contact mode operation is illustrated in Fig. 2. A temperature bias between the proximal TC junction and the sample causes thermal conduction across the air gap and along the probe shank. Due to the large thermal resistance of air gap, a significant fraction of the temperature bias may be dropped across it. The remainder that is dropped along the probe shank between the two TC junctions is responsible for the readout signal. In non-contact mode the thermal probe can be used to map topography because the readout signal responds to variations in the air gap, as indicated by the dashed lines in Fig. 2. The large thermal resistances of the air gap and the probe shank generally prevents the probe from thermally loading the sample, despite any temperature bias that may exist. Contact mode operation can be evaluated as a special case of non-contact operation in which the thermal resistance between the tip and the sample is relatively small and does not track the topography. Models for interaction between the scanning tip and sample are the subject of active research [Ham96, Luo97, Dep97, Gom98].

A comparison of probes with different dimensions and structural materials is afforded by the simple equivalent circuit model is illustrated in Fig. 3. In this, R_{sh} and C_{sh} represent the distributed thermal resistance and capacitance of the probe shank, and include the structural material as well as the embedded thermocouple materials. The resistance of the air gap is labeled R_g. Its lower limit, which is relevant only in contact mode, is constrained by the effective contact and spreading resistance at the probe tip. For a given R_g, the temperature sensitivity of the probe can be increased by increasing R_{sh}, and the response speed of the probe can be reduced by reducing the product $R_{sh}C_{sh}$. In order to optimize these two performance criteria, therefore, the structural material of the probe should have the lowest thermal conductivity and the specific heat capacity *for the dimensions used.* Polyimide offers an important advantage over other structural materials in this respect.

The simulated responses of Si, SiO_2, and polyimide shank probes are compared in Table I. The probes dimensions assumed were 200 μm length and 40 μm width, with 3 μm thickness for the polysilicon and polyimide probes, and 0.5 μm thickness for the oxide probe. The TC was assumed to be comprised of one 10 μm wide, 2000 Å thick trace of Ni and another of W. The thermal resistance R_g was 120,000 K/W, estimating contact and spreading resistance in touch mode operation. In response to a step change in the temperature difference between the proximal TC junction and the sample, (represented in Fig. 3 by T_{Bias}), the final temperature drop achieved across the thermocouple (T_{TC}) was determined, along with its 10% to 90% rise time (t_r). The results show that the high thermal resistance of the polyimide probe shank offers almost one order of magnitude higher sensitivity than a Si probe of equal thickness. It is also more sensitive than an oxide probe which is much thinner. However, the increased thermal resistance of the polyimide probe results in a slower response, which is reduced by a factor of 5 compared to the Si probe. For the intended applications, this is a favorable compromise.

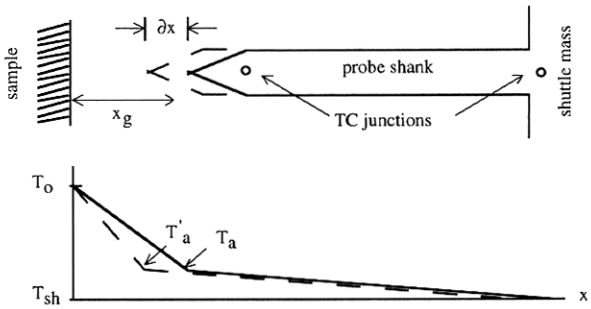

Fig. 2. A simplified thermal model illustrating the operation of a thermal probe.

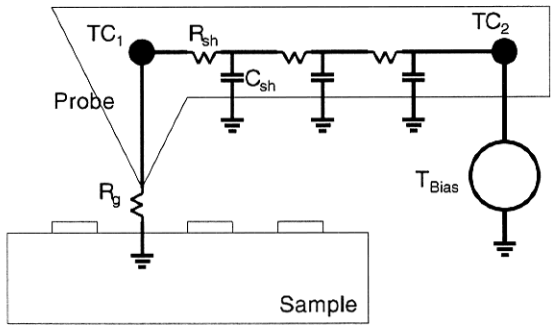

Fig. 3. Thermal conduction model for simulations. R_{sh} and C_{sh} represent distributed thermal elements that are composites of structural and TC materials of the probe.

Table I. Material properties and simulations results of thermal probes with Si, SiO_2, and polyimide shanks. T_{TC}(DC) is the DC percentage drop of T_{Bias} along the probe length, while t_r is the 10%-90% rise time of the temperature in response to a step change in T_{Bias}.

Parameter	*Si*	*SiO_2*	*PI 2610*
T_{TC}(DC)	9.7	75.4	81
t_r (ms)	0.44	1.2	2.26
Th. Cond. (W/mK)	141.2	1.4	0.147
Sp. Heat Cap. (J/gm-K)	0.7	1.4	1.09
Density (gm/cc)	2.33	2.19	1.4

III. FABRICATION

The fabrication process uses 6 masks and requires (100) oriented Si substrate wafers (Fig. 4). An oxide masked anisotropic wet KOH etch is first used to define a pyramidal notch into which the tip will be molded. The opening is sized to allow a self-terminating etch that is 5-6 μm deep. This is designed to prevent interference from

the overhang of the cantilever past the tip while scanning. A 2 μm thick sacrificial layer of Ti is deposited and patterned using a photoresist masked 30 second wet etch in 5% HF. The Ti is retained over the area in which the probe will be released. The first polyimide layer is then spun on, cured, and patterned, removing it from the field regions and from within the notch. DuPont's Pyralin™ PI2610 is suitable because its coefficient of thermal expansion (3 ppm/K) is close to that of Si, which minimizes the curl in the released probe shank. An Al hard mask is used with a dry reactive ion etch of O_2 and SF_6 to pattern the polyimide. The TC metals are deposited and patterned in the following two masking steps. One side of the TC is Cr/Ni 200/2000 Å, while the other is 200/2000/200 Å Cr/W/Cr. The Cr/Ni layer also forms the integrated heating resistor. (Ni may be replaced by Au for tunneling microscopy applications.) The lower Cr layer serves to improve adhesion in both Ni and W, whereas the upper Cr layer used with W is for protection against the subsequent dry etch of the second polyimide layer, which is spun on, cured and patterned by a dry etch immediately after. This dry etch terminates on the sacrificial Ti in the field and on the Cr/W/Cr layer on the TC pads. Finally, the probe is released and manually flipped over. An optional Cr wet etch can be performed after release to strip the layers covering the exposed scan tip and the TC and resistor pads. An unreleased probe is shown in Fig. 5, and released probes before and after they are flipped over are shown in Fig. 6.

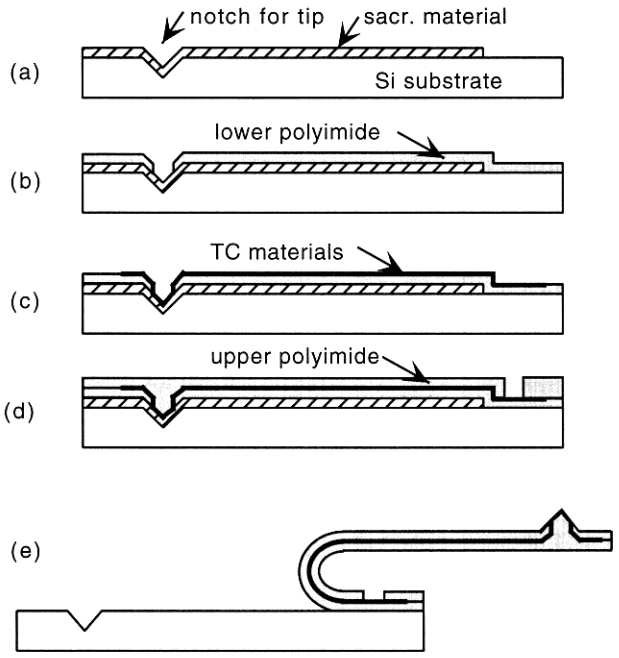

Fig. 4. Fabrication sequence: (a) Tip notch is etched into silicon wafer and sacrificial layer is deposited and patterned (masks 1, 2); (b) First polyimide is deposited and patterned, removing it from the field region and within the tip notch (mask 3); (c) TC materials are deposited and patterned (masks 4, 5); (d) Second polyimide is deposited and patterned (mask 6); (e) Sacrificial layer is etched, and the probe is flipped over and clamped in new position.

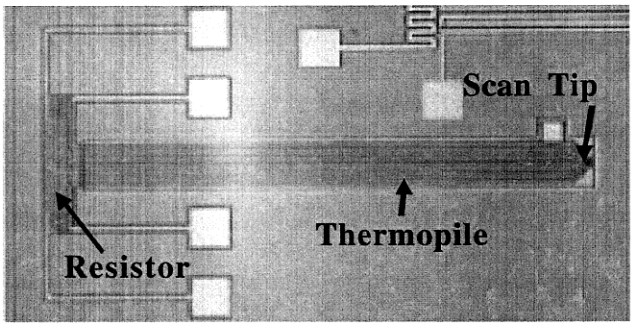

Fig. 5. Optical micrograph of a fabricated thermal probe immediately before release.

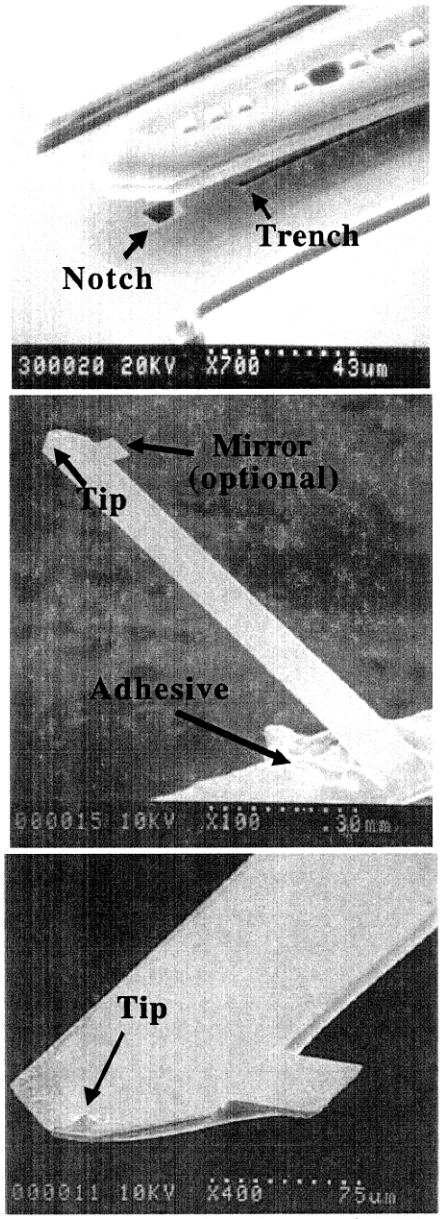

Fig. 6 (a: top – c: bottom). SEM images of: (a) A scanning probe tip, immediately after release from the mold; (b) An 800 μm long probe flipped over the die edge and held down with epoxy; (c) A close-up of the probe shank, showing the scan tip and the paddle-shaped mirror.

It should be noted that once the oxide mask for the KOH has been deposited in the first step of this process, the highest temperature encountered is the 350°C cure for polyimide.

The diameter of the scanning tip is determined by the sharpness of the notch in substrate within which it is formed. A self-terminating anisotropic wet etch in which the mask opening is aligned to the crystallographic axes of the substrate wafer provides a tip diameter of 100-200 nm, as shown in Fig. 7. Although this is adequate for many applications, the tip diameter can be reduced to about 10 nm by thermally oxidizing the notch prior to depositing the sacrificial Ti [Suz96].

The use of polyimide as a structural material permits the thickness of the probe shank to be scaled in the range of 1-20 μm as a variable for adjusting the spring constant of the cantilever. For several of the devices reported here, each of the two polyimide layers was ≈1.55 μm thick PI2610. For a 200 μm long, 40 μm wide probe, this yields a spring constant of 0.31 N/m, whereas for a 1000 μm long, 120 μm wide probe, it yields 7.4×10^{-3} N/m. Another option for adjusting the shank stiffness is to mold a longitudinal rib on its underside. This can be done without any additional processing steps by etching a narrow trench along the length of the shank during the formation of the notch for the scan tip. Making the trench narrower than the notch ensures that it is also shallower than the notch, so the polyimide rib molded by it does not protrude beyond the scan tip once the probe is flipped over. This is necessary because the rib might otherwise potentially interfere with a scan. A close-up of the trench and the notch underneath a released probe are shown in Fig. 6a.

IV. MEASUREMENT RESULTS

The first step in characterizing a fabricated thermal probe is to measure the temperature coefficient of resistance (TCR) of the integrated heater. The resistor is uniformly heated by an external source while its resistance is monitored as a function of temperature. A typical response plot showing a TCR of 4282 ppm/K is provided in Fig. 8.

The next step is to measure the response of the TC or thermopile using the integrated resistor [Gia97]. For this the distal junction of the TC is held at room temperature by bringing the scanning tip of a released probe into contact with a relatively large, thermally conductive mass. Meanwhile, a current is passed though the integrated heater, elevating the temperature of the proximal junction. Since the temperature of the heater is known from the change in its resistance, the TC output can be observed as a function of the temperature difference between the hot and cold junctions. The typical response of a Ni/W thermopile is plotted in Fig. 9. Other materials may be used for higher sensitivity as long as process compatibility is not an issue.

The polyimide probe characterized in Fig. 9 was used in a contact mode scan of the sample in Fig. 10. The scanned area was a portion of a 263 Ω metal resistor patterned on a Si substrate and isolated from it by a 4 μm thick layer of polyimide. A DC current of 4 mA was passed through the resistor. The thermopile output, presented in Fig. 11, shows a temperature rise of about 5°C. The peak is located near the apex formed by the bend between the two linear segments of the resistor, which are 10 μm wide and 20 μm apart where they run parallel to each other. The contact force between the tip and the sample for this measurement, estimated from the bending of the probe, was in the range of 30-50 nN.

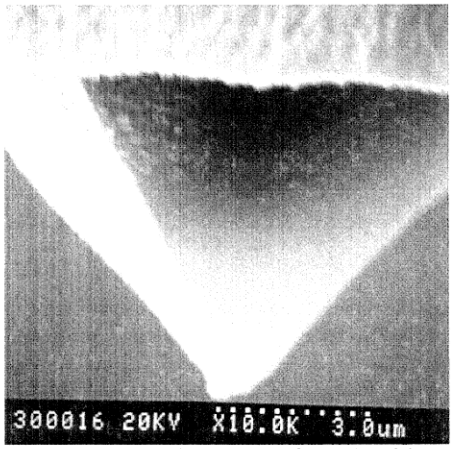

Fig. 7. A close-up of the tip formed without oxide-sharpening the mold.

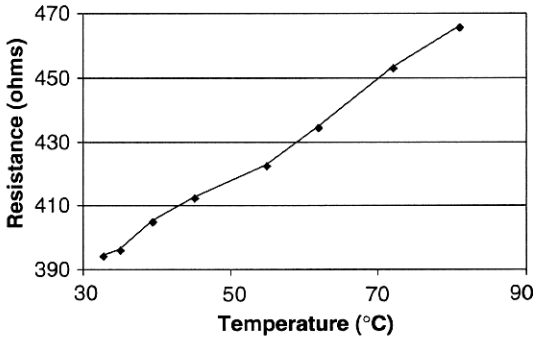

Fig. 8. Measured results for the TCR characterization of a Ni resistor. The TCR of the resistor was 4282 ppm/K.

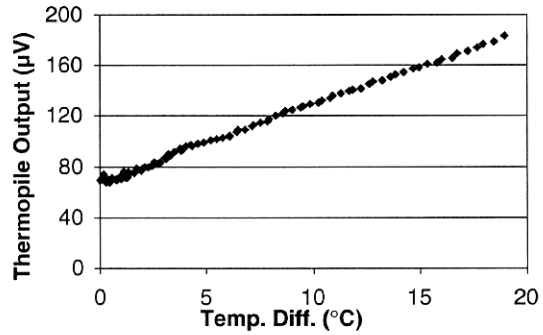

Fig. 9. Measurements of the Ni/W thermopile show 6.0 μV/K response.

The response speed or bandwidth of the thermal probe can be determined by a measurement similar to the one used for TC characterization. In this, an AC signal is applied to the integrated heater while the scan

tip is held at room temperature. Since the input power is proportional to the square of the applied voltage, a sinusoid at frequency *f* centered at ground (without a DC bias) generates power signal at *2f*, and consequently a TC output at *2f*, as shown in Fig. 12. (The presence of a DC bias will cause the power signal to have components at both *f* and *2f*, and must be avoided.) As the input signal frequency is increased, the TC is eventually unable to keep up with the power oscillations, and the amplitude of the V_1 peak in the response cycle degrades while V_2 remains unchanged. The ratio of these two peaks is plotted as a function of the power frequency, *2f*, as in Fig. 13. These measurements were performed on a 200 μm long, 40 μm wide TC probe, and a 1000 μm long, 120 μm wide thermopile both of which were 3.1 μm thick. The input signal for the TC and the thermopile were 5 V and 3 V peak-to-peak amplitudes, respectively. Both output signals showed a –3 dB bandwidth of about 500 Hz, suggesting that the scan speed should not exceed 2 ms per pixel for these probes.

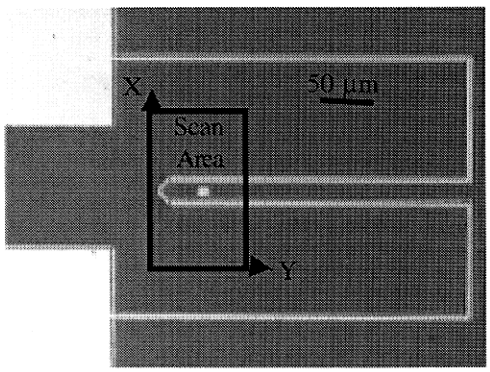

Fig. 10. Micrograph of the scan sample used in Fig. 8, showing a 263 Ω metal resistor patterned on top of 4 μm polyimide on a Si substrate. A DC current of 4 mA was applied to the resistor.

Fig. 11. The scanned thermal image of the resistor in Fig. 10 with the thermopile response on the vertical axis. The scan clearly shows that the apex of the sample resistor is hotter than the surrounding areas.

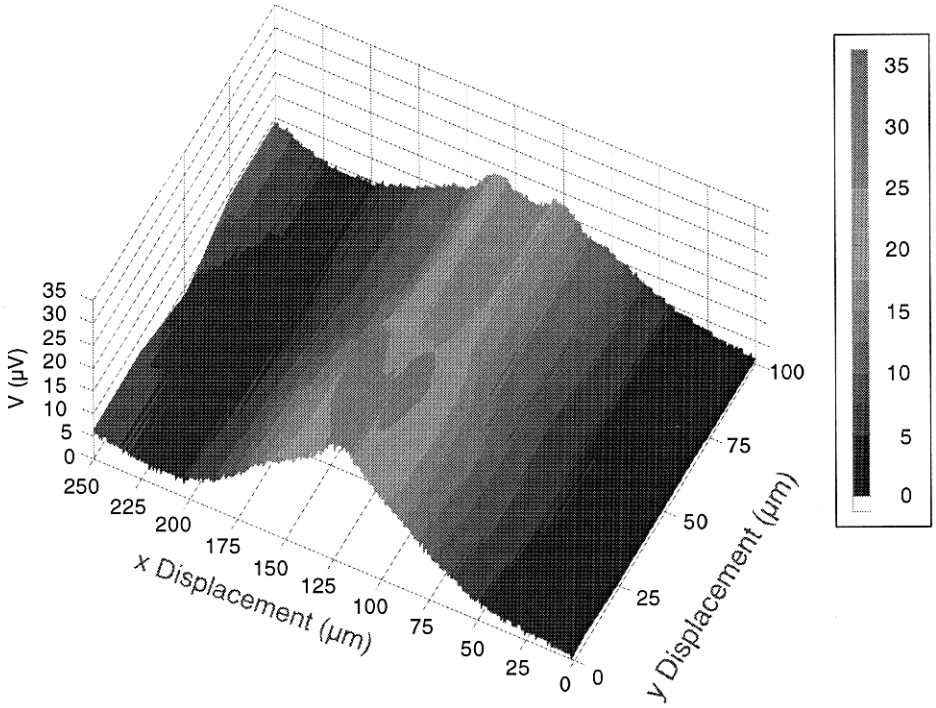

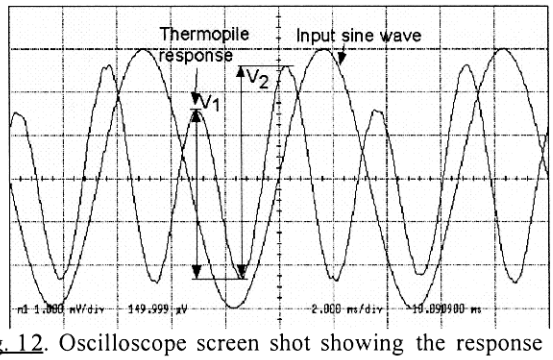

Fig. 12. Oscilloscope screen shot showing the response of a released thermopile probe to a sine wave applied to the heater. The 150 Hz input voltage generates power oscillations at 300 Hz, reflected by the thermopile response.

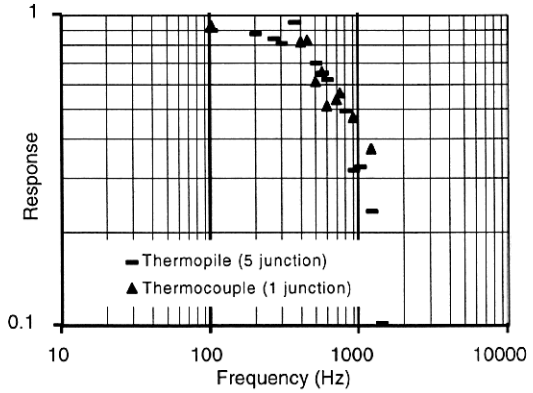

Fig. 13. Bandwidth measurements of thermocouple and thermopile probes show a corner frequency of ≈500 Hz.

V. CONCLUSION

This effort has described polyimide-based scanning thermal profilers with integrated tips and embedded thin-film thermopiles for temperature sensing. Although polyimide is rarely the best choice for a structural material in MEMS, the very low thermal conductivity and the very high mechanical flexibility that it offers are critical advantages to these devices. Simulations suggest that using polyimide as a structural material increases the temperature sensitivity of a probe by about 10x compared to a Si probe of the same dimensions. The response speed is reduced by about 5x, which is an acceptable compromise. The polyimide probes are surface micromachined on a Si substrate using a low-temperature 6-mask process suitable for appending to a CMOS process sequence. They are assembled by a unique flip-over approach, allowing the scanning tip to overhang the edge of the chip for easy alignment to the sample and for optical access to a laser. The probes, which may be used for force and tunneling microscopy as well, are 200-1000 μm long, 40-120 μm wide and of varying thickness. Tip diameters are in the range of 200 nm, but can be sharpened to about 10 nm without the use of additional lithography steps. The integrated thin film Ni/W thermopiles offer a temperature sensitivity of about 6 μV/K. Other materials may be used for higher sensitivity within the constraints of process compatibility. Scan results of a 263 Ω wire carrying 4 mA are presented. Frequency response measurements of a 200 μm long, single TC probe and a 1000 μm long, thermopile probe both show –3 dB bandwidth ≈500 Hz.

ACKNOWLEDGEMENTS

This work was funded in part by the Semiconductor Research Corporation under contract no. 98-LP-452.005. The Center for Nano Technology, UW-Madison, is supported in part by DARPA/ONR grant no. N00014-97-1-0460.

REFERENCES

[Aki99] T. Akiyama, D. Lange, C. Hagleitner, A. Tonin, O. Brand, H. Baltes, U. Staufer, N.F de Rooij, "Active and self-detecting cantilever with on-chip CMOS electronics for scanning force microscopy," *Proc., IEEE International Conf. on Sensors and Actuators (Transducers 99),* pp. 1848-51, Sendai, Japan.

[Ata93] M. Ataka, A. Omodaka, N. Takeshima, H. Fujita, "Fabrication and operation of polyimide bimorph actuators for ciliary motion system," *J. Microelectromechanical Sys.*, 2(4), pp. 146-50, '93.

[Dep97] F. Depasse, S. Gomès, N. Trannoy, Ph. Grossel, "AC thermal microscopy: a probe-sample thermal coupling model," *J. Phys. D: Appl. Phys.*, 30, pp. 3279-85, 1997.

[Fry98] D. Fryer, J. de Pablo, P. Nealey, "Investigation of photoresist/wafer interface with a local thermal probe," *SPIE,* vol. 3333, pp. 1031-9, 1998.

[Gia97] Y.B. Gianchandani, K. Najafi, "A silicon micromachined scanning thermal profiler with integrated elements for sensing and actuation", *IEEE Transactions on Electron Devices*, 44(11), pp.1857-67, 1997.

[Gom98] S. Gomès, F. Depasse, Ph. Grossel, "3D thermal wave scattering on buried inhomogeneities in ac thermal microscopy", *J. Phys. D: Appl Phys,* 31, p. 2377-87, '98.

[Ham96] A. Hammiche, H.M. Pollock, M. Song, D.J. Hourston, "Sub-surface imaging by scanning thermal microscopy", *Measurement Science & Technology*, 7(2), pp.142-50, 1996.

[Lei98] T. Leinhos, M. Stopka, E. Oesterschulze, "Micromachined fabrication of Si cantilevers with Schottky diodes integrated in the tip", *Applied Physics A*, 66, pp. S65-9, 1998.

[Luo97] K. Luo, Z. Shi, J. Varesi, A. Majumdar, "Sensor nanofabrication, performance, and conduction mechanisms in scanning thermal microscopy", *J. Vac. Sci. Technol. B*, 15(2), pp. 349-60, 1997.

[Maj98] A. Majumdar, J. Varesi, "Nanoscale temperature distributions measured by scanning joule expansion microscopy", *Journal of Heat Transfer*, 120, pp. 297-305, 1998.

[Mil98] G. Mills, H. Zhou, A. Midha, L. Donaldson, J.M.R. Weaver, "Scanning thermal microscopy using batch fabricated thermocouple probes", *Applied Physics Letters,* 72(22), pp. 2900-02, 1998.

[Oco96] L.E. Ocola, D. Fryer, G. Reynolds, A. Krasnoperova, F. Cerrina, "Scanning force microscopy measurements of latent image topography in chemically amplified resists", *Appl. Phys. Lett.*, 68(5), pp. 717-19, January , 1996.

[Suz96] Y. Suzuki, "Novel Microcantilever for scanning thermal imaging microscopy", Jpn. J. Appl. Phys. Part 2, 35(3A), pp. L352-4, 1996.

[Tha99] J. Thaysen, A. Boisen, O. Hansen, S. Bouwstra, "AFM probe with piezoresistive read-out and highly symmetrical wheatstone bridge arrangement" *Proc., IEEE International Conf. on Sensors and Actuators (Transducers 99),* pp. 1852-5, Sendai, Japan

[Var98] J. Varesi, S. Muenster, A. Majumdar, "High-resolution current and temperature mapping of electronic devices using scanning joule expansion microscopy", *IEEE 36th Annual International Reliability Physics Symposium*, pp. 169-72, 1998.

[Wic89] H.K. Wickramasinghe, "Scanned-probe microscopes," *Scientific American,* pp. 98-105, Oct. '89

[Wil86] C. Williams, H.Wickramasinghe, "Scanning thermal profiler," *Applied Physics Letters,* 49(23), p. 1587-9, Dec. 1986